On Uncertainty Analysis and Surface Error Estimation of Cable-Mesh Structure

On Uncertainty Analysis and Surface Error Estimation of Cable-Mesh Structure

By Nozomu Kogiso[1)], Takahiro Matsuo[1)], Takeshi Akita[2)] and Hiroaki Tanaka[3)]

[1)]*Department of Aerospace Engineering, Osaka Prefecture University, Sakai, Japan*
[2)]*Department of Mechanical Science and Engineering, Chiba Institute of Technology, Narashino, Japan*
[3)]*Department of Aerospace Engineering, National Defence Academy of Japan, Yokoshuka, Japan*

A cable-mesh structural configuration is one of the light-weight structural concepts adopted on a kind of space structures such as a large-scale deployable reflector consisting of the surface and back-up cable meshes and tie-cables. The surface shape is stabilized by applying appropriate tensional load to the surface cables and supported tie-cables. Variations on cable tensional force due to uncertainties on cable natural length or Young ’ s modulus will deteriorate the surface shape accuracy that is one of the most important factors on the space reflector. In addition, sophisticated adjusting approach to control the surface shape with less effort is required. For the purpose, this study addresses the uncertainty analysis on a typical type of a cable-mesh reflector consisting of 930 surface cables and 325 tie-cables that is designed to satisfy less than 3×10^{-4} mmRMS surface error on the nominal condition. As a preliminary uncertainty analysis, deterioration of the surface shape due to variations on natural length of tie-cables is investigated by Monte Carlo simulation. Then, the surface error is described by Zernike polynomials. The surface error modeled by the appropriate number of free parameters will make it possible to perform on-orbit adjustment of the reflector with reduced number of adjusters.

Key Words: Surface Error, Uncertainty Analysis, Cable-Mesh Structure, Zernike Polynomials

1 Introduction

A space reflector of a cable-mesh structural configuration shown in Fig. 1 consists of a mirror cables, a back-up cables as counterparts of the mirror cables and tie cables that connect the both cables. This structural configuration was developed to achieve the surface mirror accuracy requirement by loading an appropriate tension to each cable[1)] and was adapted in HALCA satellite [3)]. As the surface accuracy is affected by manufacturing errors such as length and stiffness of cables, adjustment of these parameters are important task before launch. HALCA satellite satisfied the shape accuracy requirement by adjusting cable lengths at the ground verification test.

A future space mission requires higher shape accuracy to observe using higher frequency electromagnetic wave. For the purpose, an efficient mechanism by reducing the number of adjustment parts is required to reduce the adjustment effort[2)]. On the other hand, uncertainties such as cable length errors or variation of cable elasticity have significant effect on the shape accuracy.

This study considers uncertainty of natural lengths of tie

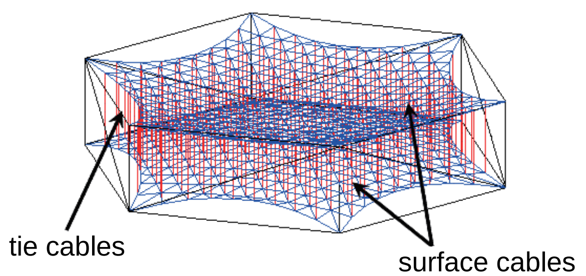

Fig. 1 Cable mesh reflector

cables and investigates the effect on the shape accuracy[4,5)] by numerical calculations using a sample cable-mesh reflector shown in Fig. 1. The cable-mesh structure consists of 930 surface cables and 325 tie-cables, and the diameter, aperture area and focal length of this reflector are about 5m, 12.28m^2, and 8m, respectively.

First, sensitivity of the surface accuracy in terms of the tie cable length is investigated. The probabilistic distribution of the surface accuracy is estimated in terms of variation of the tie cable length by Monte Carlo simulation. Then, the variation of the surface shape is estimated using Zernike's polynomials[6)] that are used to model variation of wave surfaces such as defocus, astigmatism, or coma aberration modes of the optical systems. The orthogonal polynomials are applied to model surface errors of the space antennas[7)]. In addition, adjustment of the surface error on orbit is expected.

2 Variation of RMS Error Caused by Tie Cable Length Uncertainty

In this study, deformation shape and internal force distribution of the cable-mesh reflector are evaluated by using an in-house nonlinear FEM code developed by one of the author. The flow of the nonlinear FEM analysis is illustrated in Fig. 2. Newton-Raphson method with a line-search is adopted to update the tangent stiffness matrices.

Each cable length of the cable-mesh reflector shown in Fig. 1 is designed to have an 8m focal length parabola surface for the nominal equilibrium condition. For the nonlinear FEM analysis, the surface error is found to be 2.81×10^{-4}mmRMS.

2.1 Variation of RMS Error

When the tie cable length, l_i is shifted from the nominal length as $l_i(1 \pm \alpha)$, the surface will deteriorate. First, the

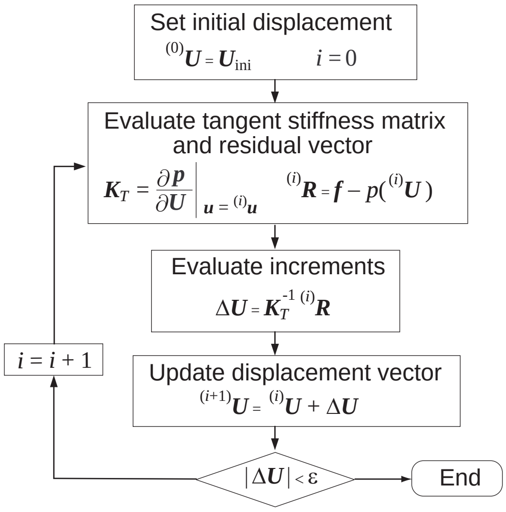

Fig. 2 Nonlinear FEM analysis flow, $\boldsymbol{f} = \boldsymbol{p}(\boldsymbol{U})$

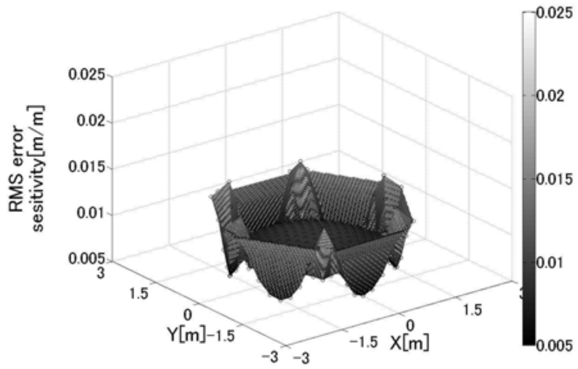

(a) In case of 1% shorter

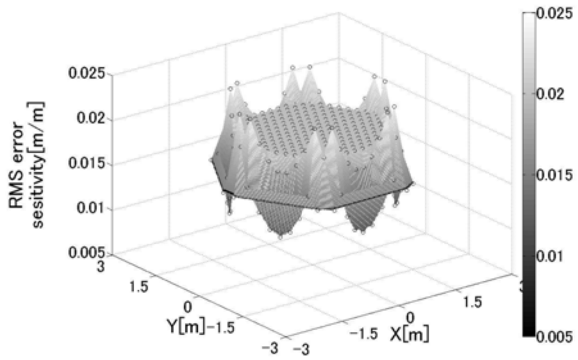

(b) In case of 1% longer

Fig. 3 RMS error distribution due to 1% variation of tie-cable length.

deteriorate rate of the surface accuracy due to variation of each tie cable length is investigated.

Fig. 3 illustrates the RMS error distributions in case of 1% longer or shorter variations of the tie cable length from the nominal condition, $\alpha = 0.01$, where (a) x–y plain indicates the position of the tie-cable, and z-coordinate the RMS error value. It indicates that the edge cables have larger effects on the RMS error than cables around the center.

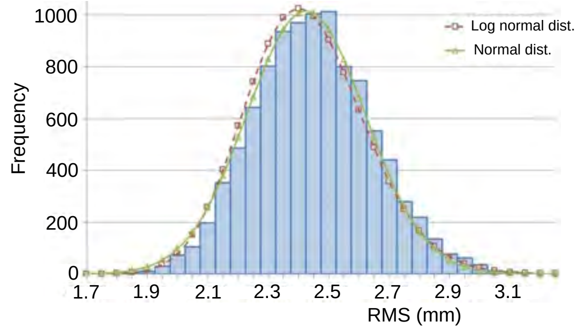

Fig. 4 Histogram of RMS error obtained from 10000 samples under 1% of coefficient of variation

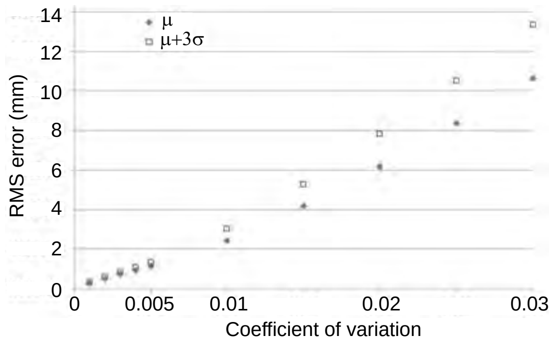

Fig. 5 RMS errors in terms of the coefficient of variation of the tie cable length.

2.2 Monte Carlo Simulation

Then, statistical property of variation of RMS error caused by the tie cable length uncertainty is estimated by Monte Carlo simulation. Assume that the tie cable lengths are independent normal distribution with 1% of coefficient of variation, standard deviation divided by average value, where the average values are assumed to have nominal values. Histogram of the RMS error obtained by Monte Carlo simulation with 10000 samples is illustrated in Fig 4. It is estimated that the RMS error (mmRMS)is normally distributed of the average $\mu = 2.42$ and standard deviation, $\sigma = 0.196$. It indicates that uncertainty of the RMS error can be described as a linear function in terms of variations of the tie cable length.

Then, the averages and the standard deviations are investigated for different values of coefficient of variation. Fig. 5 shows the change of average μ and the worst value $\mu + 3\sigma$ in terms of the coefficient of variation. The average and the standard deviations are linearly varied in terms of the coefficient of variation, when the value is less than 1%. On the other hand, the slope is changed at around 1% of the coefficient of variation. That means, some nonlinear effect will appear on the variation of RMS errors.

3 Shape Error Described Using Zernike Polynomials

Zernike polynomials are widely used in the analysis of optical phase properties as reflectors [7]. In this study, the shape error is represented by using these polynomials to relate the error to the optical mode. The polynomials are defined as follows:

$$U_{n,m}(r, \theta) = R_{n,m}(r)\cos(m\theta) \qquad m \geq 0 \qquad (1)$$

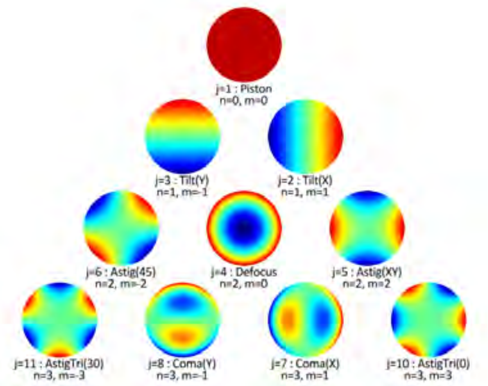

Fig. 6 Lower Zernike modes[8].

$$U_{n,m}(r,\theta) = R_{n,m}(r)\sin(|m|\theta) \qquad m < 0 \qquad (2)$$

Where

$$R_{n,m}(r) = \sum_{s=0}^{(n-|m|)/2} \frac{(-1)^s (n-s)!}{s!\,\{(n+m)/2 - s\}!\,\{(n-m)/2 - s\}!} r^{n-2s} \qquad (3)$$

Some lower modes correspond to tilt, defocus astigmatism, coma shown in Fig. 6.

The shape error $Z(r,\theta)$ is approximated by describing weighted sum of $U_{n,m}(r,\theta)$.

$$Z(r,\theta) = A_1 U_{0,0}(r,\theta) + A_2 \boldsymbol{U}_{1,1}(r,\theta) + \cdots + A_k \boldsymbol{U}_{n,m}(r,\theta) \quad (4)$$

where $A_i, (i = 1, \cdots, k)$ is a weighting coefficient corresponding to each term.

A sample example of the shape error distribution obtained from Monte Carlo simulation in the previous section is illustrated in Fig. 7 (a). The approximated shape error by Zernike polynomials is shown in Fig. 7 (b). It is found that the approximation works well when the higher modes are adopted, where the RMS error is 0.509 mmRMS and the coefficients are shown in Fig. 7 (c).

Then, the statistical property of the Zernike approximation is demonstrated from 10000 Monte Carlo simulation samples described in the previous section. The average, standard deviation and the absolute value of coefficient of variation (c.o.v.: deined as standard deviation devided by average) of Zernike polynomial coefficients are shown in Fig. 8, where 400 Zernike terms are used in the approximation. The dominant terms are listed in Table 1, where terms with $m = 0$ correspond to the circular modes and those $m = 6k$ (mode multiplies of six) to the hexagon modes. The hexagon modes have significant effect on this reflector, because this reflector is a hexagon-based shape. In addition, some modes have large standard deviations in spite of small average values. Considering uncertainties of the tie cable length, attentions should be paid on such modes.

4 Concluding Remarks

This study investigates effects of uncertainty of the tie cable length of the cable-mesh reflector on the shape accuracy. Through the sensitivity analysis, variation of the shape RMS error caused by the tie cable length uncertainty is investigated and the statistical property is investigated through Monte Carlo simulation. Then, the shape error is approximated by using Zernike polynomials. The dominant modes caused by uncertainties are also demonstrated.

Based on this approach, effect of uncertainty of the thermal environment on orbit on the shape accuracy [9,10] and the efficiency of Zernike polynomials will be investigated.

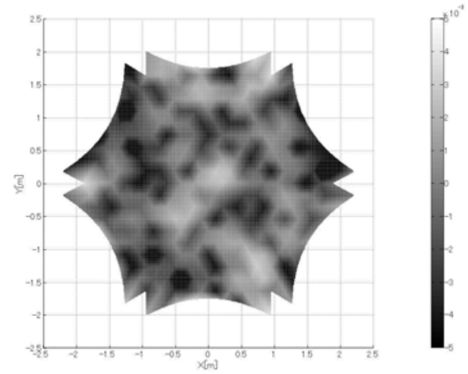

(a) Surface error distribution example.

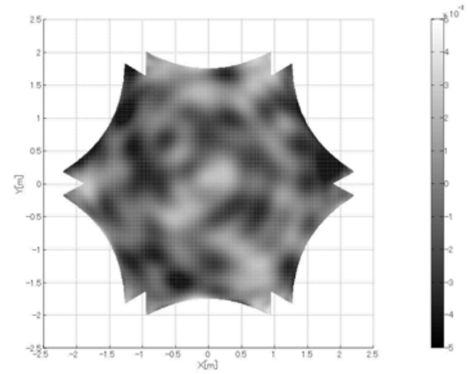

(b) Approximation using Zernike polynomials.

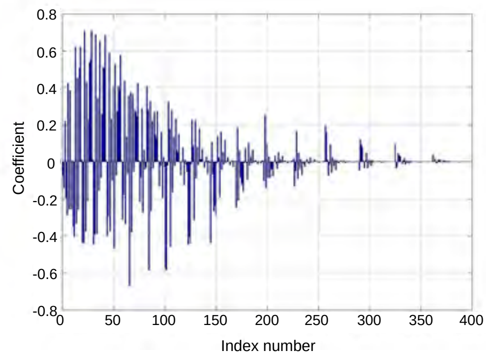

(c) Coefficients of Zernike polynomials.

Fig. 7 Surface error distribution and its approximation.

Acknowledgments

This study was supported by "Advanced Light-weighted Structural System Research" in the "Strategic Development and Research Fund" of ISAS/JAXA (Institute of Space and Astronautical Science, Japan Aerospace Exploration Agency).

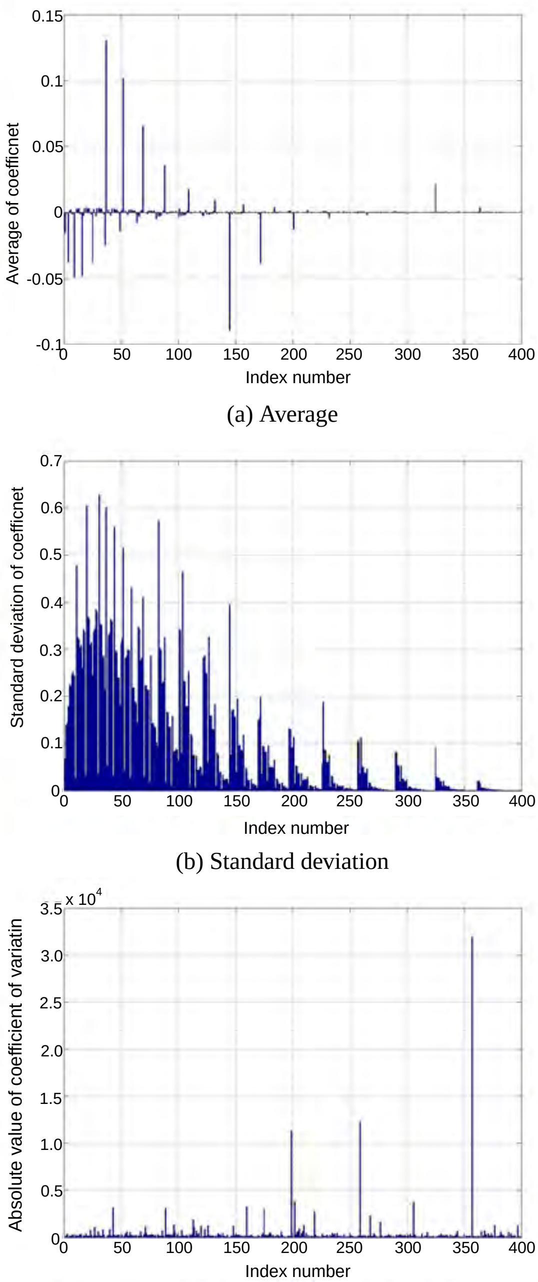

(a) Average

(b) Standard deviation

(c) Absolute value of coefficient of variation

Fig. 8 Zernike coefficients obtained from 10000 samples under 1% coefficient of variations of tie cable length.

Table 1 Dominant Zernike terms.

Index	n	m	Average ($\times 10^2$)	Standard deviation ($\times 10^2$)	c.o.v.
1	0	0	-1.57	6.59	4.20
325	18	18	2.17	9.21	4.25
145	12	12	-8.97	39.36	4.39
37	6	6	13.01	60.09	4.62
364	20	18	0.32	1.49	4.64
4	2	0	-3.77	17.86	4.74
9	4	0	-4.92	24.25	4.98
52	8	6	10.15	51.57	5.08
172	14	12	-3.85	19.85	5.15
16	6	0	-4.83	26.07	5.39
⋮	⋮	⋮	⋮	⋮	⋮

References

1) Tanaka, H., and Natori, M. C.: Shape Control of Space Antennas Consisting of Cable Networks, *Acta Astronautica*, **55**-3-9 (2004), pp. 519-527
2) Tanaka, H.: Design Optimization Studies for Large-Scale Contoured Beam Deployable Satellite Antennas, *Acta Astronautica*, **58**-9 (2006), pp. 443-451.
3) Takano, T., *et al.*: Deployable Antenna with 10-m Maximum Diameter for Space Use, *IEEE Transactions on Antennas and Propagation*, **52**-1 (2004), pp. 2-11.
4) Tanaka, H.: Surface Error Measurements of Reconfigurable Antennas Based on Antenna Gain Analyses, *Space Technology Japan*, **7** (2008), pp. 19-25 (in Japanese).
5) Tanaka, H.: Surface Error Estimation and Correction of a Space Antenna Based on Antenna Gain Analyses, *Acta Astronautica*, **68**-7-8 (2011), pp. 1062-1069.
6) Born, M. and Wolf, E.: *Principles of Optics: Electromagnetic Theory of Propagation, Interference and Diffraction of Light*, 7th ed., Cambridge University Press, London, 1999.
7) Toyoshima, M., *et al.*: Mutual Alignment Errors Due to the Variation of Wave-Front Aberrations in a Free-Space Laser Communication Link, *Optics Express*, **9**-11 (2011), pp. 592-602.
8) Zernike Mode Map, `http://www.lambda-factory.co.jp`
9) Usui, M., *et al.*: Suppression of Thermal Deformation of the Large Deployable Reflector, *Trans. JSME, C*, **77**-777 (2011), pp. 487-499, (in Japanese).
10) Hill, J. R., Wang, K. W., Fang, H., and Quijano, U.: Actuator Grouping Optimization on Flexible Space Reflectors, Proc. SPIE 7977, Active and Passive Smart Structures and Integrated Systems, 2011, 797725